A Hierarchical Registration Algorithm for Fingerprints from Multi-type Capture Sensors

Yali Zang†, Xin Yang†, Xiaofei Jia, Ning Zhang, Jie Tian*
Institute of Automation, Chinese Academy of Sciences, Beijing 100190 China

Xinzhong Zhu
College of Mathematics Physics and Information Technology, Zhejiang Normal University

†These authors contribute equally to this work. *Corresponding author: tian@ieee.org

Abstract

Various types of fingerprint sensors introduce large variances of fingerprints in distortion patterns and noise, which greatly challenge the traditional matching algorithms. In this paper, we develop a hierarchical registration algorithm to handle the non-linear distortion among multiple kinds of sensors. The transformation model is initially estimated with the traditional rigid model and gradually upgraded to affine and quadratic model. The model upgradation is carefully designed to obtain the trade-off between the fitting accuracy of high-level model and the facilities of low-level model. We finally establish the minutiae correspondence with a modified ICP (Iterative Closest Point) method. Experimental results demonstrate that our algorithm effectively improves the performance of cross-matching, especially for those databases in different modes of acquisition.

1. Introduction

Fingerprints have been increasingly used for individual identification in the governmental and civil application. Recently great improvement has been achieved in the fingerprint sensing technology and automatic recognition algorithms. According to sensing principles, these sensors can be divided into optical, capacitive, thermal or ultrasonic ones. According to the mode of capture manner, they can be classified into press(rolled, flat and slap), sweep and non-contacted ones. We define the matching of fingerprints from multi-type sensors as "cross-matching" in contrast to "regular matching". As far as we know, most fingerprint matching algorithms in current fingerprint application can only operate on the specific kind of sensors, enduring poor performance on different sensors. The difference among multi-type sensors will significantly affect the characteristics of the raw data, the extracted features and the similarity score generated by matching algorithm. It is necessary to develop the matching algorithms which are robust to the characteristics of sensors including resolution, capture modes, noise and so on.

As far as we know, only a few algorithms have considered the variations of fingerprints in the cross-matching. Ross et al. [11] proved that when the compared fingerprints originated from two different sensors the performance of the matcher drastically decreased. Ross et al. [12] utilized a non-linear calibration scheme to handle variations in minutiae distributions across multiple press sensors. Ross et al. [10] estimated the average TPS deformation model between each template impression and the rest of the impressions of that finger. Kovács-Vajna [6] proposed to cope with the strong deformation of fingerprint images due to static friction or finger rolling based on triangular matching, and finally validated the matching by Dynamic Time Warping.

The algorithm proposed in this paper focuses on non-linear distortion in fingerprint cross-matching. A hierarchical registration process is utilized to determine the parameters of transformation model. We aim to seek the optimal 2D model to describe the non-linear distortion caused by different acquisition patterns. Experiments are conducted to testify the effectivity of our algorithm to the variations of multi-type fingerprints.

The rest of the paper is organized as follows: Section 2 gives the preprocessing stages of the fingerprints. Section 3 describes the process of hierarchical registration. The experimental results of our algorithm are displayed in Section 4 and Section 5 summarizes our researches and future works.

2. Preprocessing and Feature Extraction

The original fingerprint images is first segmented from the background [3]. Then the gradient-based approach [4] is used to compute the orientation. The Gabor filter is applied to enhance the fingerprint with the advantages of its ro-

bust ridge enhancement and efficient noise removing. Then the fingerprint skeleton is obtained by thinning the binary ridges. A series of postprocessing steps are produced to cut short branches, remove holes and delete spurious minutiae [8]. Finally minutiae are extracted from fingerprint skeleton.

3. Fingerprint Registration

The registration stage is to transform one of the compared fingerprints in order to make its features mostly overlap the corresponding features in another fingerprint. We aim to register any pair of fingerprints with the optimal transformation model to handle the different distortion patterns of multi-type sensors.

Tab. 1 displays a three-level structure of transformation models. Each level of the hierarchy involves one transformation model in ascending order by accuracy and degree of freedom (DOF). The rigid model with 4 parameters is easy to estimate based on minutiae comparison but not robust enough for cross-matching. In contrast, the quadratic model with 12 parameters is accurate to describe the nonlinear distortion but sensitive to mismatched minutiae pair. It is difficult to directly estimate its parameters based on the compared minutiae set. The affine model with 6 parameters compromise the accuracy and facility of transformation estimation.

The most challenging problem in registration is to find the corresponding minutiae pairs from compared fingerprints. The traditional minutia-based matching seek the set of corresponding minutiae pairs with the traditional rigid model. The registration methods based on rigid model are subject to variation in finger placement and resolution difference during different acquisition. It cannot handle the global non-linear distortion caused by different acquisition modes. However, this model is still appropriate for describing the transformation in small region since distortion affects much less in the local region. In our method, the rigid model is used to initialize registration within a small region. Then its parameters are estimated based on the comparison of local minutiae pairs. We keep spanning the region until it covers the entire overlapped area, meanwhile, the model is upgraded into affine and quadratic model. The so-called model upgradation aims to optimize the tradeoff between the fitting accuracy of high-level model and the facilities of low-level model.

The following variables will be used in the registration procedure. Let $M_t \in \{rigid, affine, quadratic\}$ denote the transformation model and R_t denote the registration region in the input fingerprint at the t iteration of model upgradation. θ_t is the parameter matrix of transformation model M_t. C_t is the current set of corresponding minutiae pair within the registration region. $M_t(\theta_t, p)$ is the transformation function mapping the input minutiae p to the coordinate of template fingerprint.

3.1. Initialization with Rigid Model

Before registration, we first estimate the scale of the two compared finerprint based on ridge distance map, which is obtained by the spatial approach [7]. Then the corresponding minutiae pairs are chosen by the method in Ref. [14] with the difference that the radius of the minutiae descriptor is recomputed by scale. S_{p_i,q_k} is the similarity of minutiae p_i and q_k) from the input and template fingerprints measured by minutiae descriptor. $P(p_i, q_k)$ is the possibility of correspondence between a minutiae pair (p_i, q_k), measured by not only their similarity but also their distinctness from other minutiae in comparison respectively.

$$P(p_i, q_k) = \frac{S^2_{p_i,q_k}}{\sum\limits_n S_{p_i,q_n} + \sum\limits_m S_{p_m,q_k} - S_{p_i,q_k}} \qquad (1)$$

We start registration from the minutiae pair of the largest corresponding possibility with the rigid model. The registration region R_1 is initialized as the circular scope of the input adjacent minutiae structure with the radius $r_1 = R_p$ (R_p is empirically set 5 times as large as the global ridge distance). Then we can obtain the initial set of corresponding minutiae C_1, consisting of this minutiae pair and their adjacent matchable minutiae pairs. The parameters of translation and rotation are calculated as the average difference of location and orientation for all the minutiae pairs in C_1.

3.2. Model Upgradation

In Sec. 3.1 we have obtained the initial set of corresponding minutiae C_1 within the initial registration region R_1. Then the circular region is gradually spanned to involve more minutiae by increasing the value of its radius, meanwhile, the model is upgraded into affine and quadratic model. The procedure of model upgradation is described as following:

Step1. The initial registration, $t = 1$, M_1 is initialized as rigid model, C_1 is the set of corresponding minutiae in the circular region R_1 with radius r_1.

Step2. If the region has covered the entire overlapped region, the procedure ceases. Otherwise, the radius of the registration region r_t is increased into r_{t+1} by a certain value Δr, and $t = t + 1$.

Step3. For each minutia p_i in R_t, its closest corresponding minutiae q_k which are in the current circular region is found by a modified ICP (Iterative Closest Point) principle. Compared with the classic ICP method, we add the similarity of minutiae as an important weighting factor to diminish the impostor correspondence of minutiae. We define the feature distance function as $d(p_i, q_k) = \psi(S(p_i, q_k)) * \|M(\theta_t, p_i) - q_k\|$. $\psi(s) = (1-s^2)^2, s \in [0, 1]$

Table 1. Three Transformation Models in Fingerprint Registration. $X(\mathbf{p}) = [1, x_p, y_p, x_p^2, y_p^2, x_p y_p]^T$.

Model	$M(\theta, \mathbf{p})$	DOF	Accuracy	Stability
Rigid	$\begin{pmatrix} t_{11} & t_{12} & t_{13} & 0 & 0 & 0 \\ t_{21} & -t_{13} & t_{12} & 0 & 0 & 0 \end{pmatrix} X(\mathbf{p})$	4	low	high
Affine	$\begin{pmatrix} t_{11} & t_{12} & t_{13} & 0 & 0 & 0 \\ t_{21} & t_{22} & t_{23} & 0 & 0 & 0 \end{pmatrix} X(\mathbf{p})$	6	medium	medium
Quadratic	$\begin{pmatrix} t_{11} & t_{12} & t_{13} & t_{14} & t_{15} & t_{16} \\ t_{21} & t_{22} & t_{23} & t_{24} & t_{25} & t_{26} \end{pmatrix} X(\mathbf{p})$	12	high	low

called Beaton and Tukey weighting function [1] monotonically decreases to zero with the increasing of similarity. It weighs the Euclidean distance between p_i and q_k after mapping p_i onto the template coordinate. If there exists $q_k = argmin_{p_i \in R_t} d(p_i, q_k)$ and $d(p_i, q_k) < d_{thr}$, the compared minutiae are considered similar and spatially close (d_{thr} is empirically set 1.6 times as large as the global ridge distance of the input image), we add (p_i, q_k) into the set of corresponding minutiae C_t. Note that we do not recalculate the value of similarity during model upgradation since the local feature is not sensitive to non-linear distortion.

Step4: We estimate the parameters matrix θ_t of the current model with linear least-squares method. The loss function is written as:

$$\theta_t = argmin_\theta E(\theta, C_t) = \sum_{(p_i, q_k) \in C_t} \|M(\theta, p_i) - q_k\|^2 \qquad (2)$$

For rigid model, we still adopt the average principle to obtain the rotation and translation value. For affine and quadratic model, SVD (Singular Value Decomposition) method [9] is proved efficient and robust to find the optimal solution. It minimizes the loss function and generates the estimation error $E(\theta_t, C_t)$. If the average estimation error is larger than a preset threshold, the procedure ceases. SVD also derives the variance matrix of the parameters in the estimation of θ_t to measure the uncertainty of the transformation model [9]. Involving more minutiae pairs into SVD method usually makes the uncertainty decrease but the estimation error increase.

Step5: If the number of corresponding minutiae is large enough (at least 3 minutiae pairs for affine model, and 6 pairs for quadratic model), we attempt to upgrade the current model M_t to its subsequent higher-level model. The high-level model may excessively twist the input features, achieving good feature overlapping in the current region but huge feature displacement outside the region. After estimation of the higher model, we adopt a simple strategy to control the possible twisting. We assume the input image is covered by a grid, the size of which is four times than the average ridge width. The grid is transformed into template coordinate with the higher model. Then we record the spatial distance and direction variables for all the adjacent nodes of the transformed grid. We calculate the variance of two variables along the original horizontal and vertical direction. Then the sum of the variance for these two variables is calculated and utilized to exclude the incorrect model upgradation. If the incorrect model is detected, this step of model upgradation is cancelled and we will use the model in the last step to calculate the similarity score. Fig. 1 displays an example of imposter cross-matching excluded with this strategy. Then go to step2;

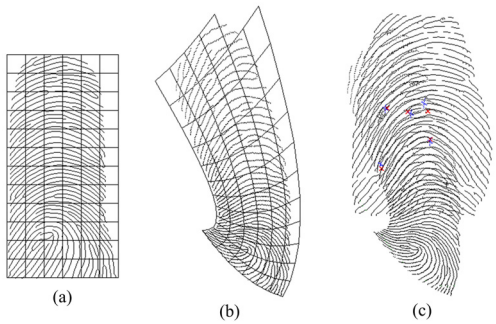

Figure 1. An example of imposter cross-matching between press sensor and sweep sensor. (a) A fingerprint skeleton covered with grid; (b) The transformed skeleton and grid with the upgraded quadratic model; (c) Overlapped fingerprints. The global image is abnormally twisted, so the upgradation is canceled.

It is worth noting that model upgradation should be done carefully. Upgrading too soon may cause model overfitting on insufficient minutiae pairs since the high-level model is more sensitive to the displacement of minutiae by noise. Otherwise, upgrading too late may cause increasing estimation error since low-level model cannot accurately describe the non-linear distortion. The upgradation is triggered when the higher-level model is preferred by comparing its estimation error and uncertainty with that of the current model [2]. The model that generates a larger value E_m will be selected.

$$E_m = \frac{d^m}{2} log(2\pi) - E + log|det(C)| \qquad (3)$$

where E is the estimation error and d_m is the dimension of model. C is the parameter estimate covariance matrix.

The radius increment of the registration region is selected to control the iterations of procedure. Small radius increment costs more time to cover the entire overlapping

Table 2. Characteristics of the chosen sub-databases.

	Capture Sensor	Image Size	DPI
DB1	URU 4000B	500*550	700
DB2	UPEK TCRU2C	208*288	508
DB3	Authentec AES2501	Unfixed	500

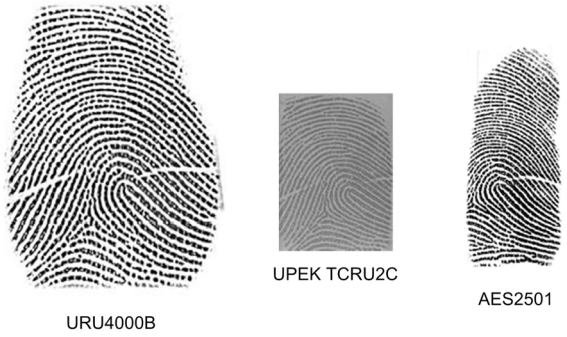

Figure 3. Three impressions from the same finger in the chosen sub-databases.

region, but it brings out more stable model estimation. In our experiments, $\Delta r = R_p$. After registration, we can obtain a set of corresponding minutiae and their local similarity. Fig. 2 displays two compared fingerprints and a series of overlapped images during the registration process, where the minutiae are paired on the modified ICP principle.

4. Experimental Results

In order to validate the performance of our algorithms, we conduct series of experiments on FingerPass database [5]. All the experiments are conducted on PC Intel Core i5 650 @ 3.20 GHZ.

4.1. Database and Evaluation Protocol

We choose three sub-databases from FingerPass, which are constructed with URU4000B optical press sensor, UPEK TCRU2C capacitive press sensor and Authentec AES2501 sweep sensor, separately. Tab. 2 describes the characteristics of these three sub-databases. Each sub-database contains 720*12 impressions (720 fingers, 12 impressions per finger). Fig. 3 gives an example including three impressions from the same finger. As analyzed in Sec. 1, press and sweep fingerprints have entirely distinguishing distortion patterns. Though both DB1 and DB2 are press sensors, fingerprints generated from them have obvious variance in resolution, noise pattern due to the different technology of optical and capacitive sensor.

The sequence of the compared fingerprints in cross-matching is arranged as following: In genuine match each impression is matched against all the impressions of the same finger to compute the False Non-Match Rate(FNMR); In imposter match the first impression of each finger is matched against the first sample of the remaining fingers to compute the False Match Rate(FMR). To sum up, a total of $103,680$ $(720 * 12 * 12)$ genuine matching and $258,840$ (C^2_{720}) imposter matching are conducted for each cross-matching. And as for regular matching, only $47,520$ $(720 * C^2_{12})$ genuine matching is done.

4.2. Experimental Design

We conduct three sets of cross-matching experiments for any two different sensors. Each set of experiments is conducted in three scenarios where the model upgradation in the registration is respectively terminated at rigid, affine and quadratic model. It is difficult to evaluate the accuracy of registration by manually. However, we can approximate its performance through the cross-matching results because the similarity score highly depends on the accuracy of minutiae correspondence derived from registration. We calculate the matching score using the typical minutiae-based matcher based on both the number of corresponding minutiae and their local similarity [13].

We also utilize thin plate spline(TPS) model to deal with the non-linear distortion in fingerprint cross-matching for comparison. Here TPS model is estimated based on the minutiae correspondences derived with the rigid model between each pair of compared fingerprints. Then it is used to pre-distort the features in the template fingerprint before matching with the input fingerprint again. Since TPS model is proved robust to describe the non-linear transformation, the pre-distortion is expected to compensate the distortion and improve the accuracy of cross-matching.

For a objective evaluation of the practicality of our algorithms for cross-matching, we compare our algorithms with a state-of-the-art commercial matcher VeriFinger 6.1 SDK [15]. We also correct the scale difference between sensors for VeriFinger SDK.

Tab. 3 summarize the comparison results of regular matching and cross-matching over all three databases respectively.

4.3. Experimental Analysis

Based on the experimental results, the following conclusions can be drawn out:

1). EERs of regular matching (whether our methods or VeriFinger 6.1 SDK-based method) are far more satisfying than those of cross-matching. Furthermore, EERs in cross-matching between the same kind of sensors (URU vs. UPEK) obviously outperforms that between different kinds of sensors (AES vs. URU, UPEK vs. AES). The comparison confirms the matching performance is greatly deteriorated by non-linear distortion and different distortion patterns.

2). Upgrading from rigid model to affine model and then

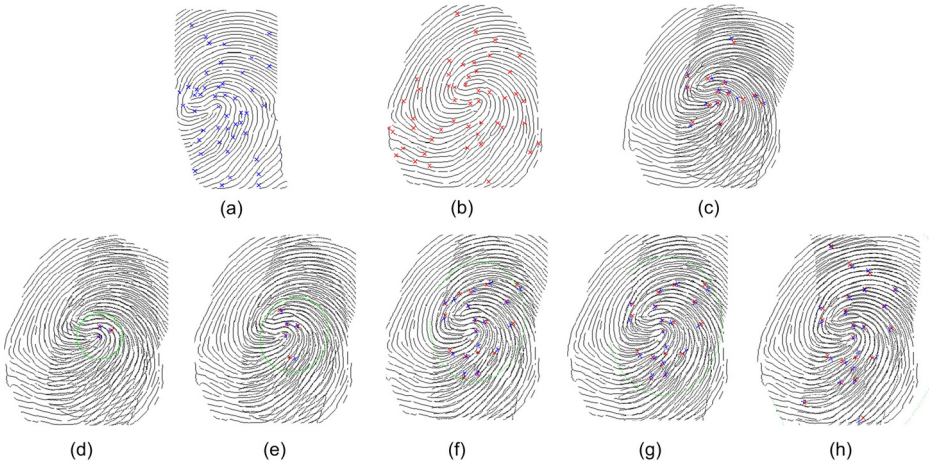

Figure 2. (a),(b) in the first row gives two compared fingerprint skeletons; (c) displays their overlapped image registered with the rigid model, where the compared minutiae whose feature distance is within a predetermined threshold are directly paired. The second row displays a series of overlapped images during the registration process. (d) with rigid model; (e),(f) with affine model; (g),(h) with quadratic model. The corresponding minutiae are marked with red and blue cross and the registration region is enclosed with a green circle.

Table 3. The performance of regular matching and cross-matching of proposed algorithms and comparison algorithms on three FingerPass databases.

	Model	EER(%)	FMR100(%)	FMR1000(%)	ZeroFMR(%)	AvgTime(s)
URU	Rigid	0.042	0.002	0.019	1.008	0.096
	VeriFinger	0.018	-	-	0.421	0.001
UPEK	Rigid	0.094	0.015	0.084	1.368	0.083
	VeriFinger	0.045	-	-	0.137	0.001
AES	Rigid	0.063	0.015	0.048	1.439	0.118
	VeriFinger	0.014	-	-	0.042	0.001
	Rigid	0.533	0.344	1.261	8.453	0.121
UPEK	Affine	0.376	0.198	0.745	5.822	0.147
vs.	Quadratic	0.231	0.079	0.342	1.803	0.178
URU	TPS	0.298	0.128	0.512	1.552	0.145
	VeriFinger	0.272	-	-	0.714	0.001
	Rigid	3.271	6.024	15.18	35.42	0.165
AES	Affine	2.562	4.326	11.33	30.81	0.193
vs.	Quadratic	2.006	3.137	9.146	16.96	0.237
URU	TPS	2.288	3.747	10.42	27.69	0.187
	VeriFinger	2.675	-	-	6.631	0.001
	Rigid	3.162	4.958	10.02	26.74	0.104
AES	Affine	2.410	3.338	7.056	17.34	0.165
vs.	Quadratic	1.799	2.071	5.201	18.28	0.217
UPEK	TPS	1.948	2.444	5.758	8.683	0.169
	VeriFinger	2.907	-	-	8.159	0.001

quadratic model does improve the accuracy of registration for cross-matching though affine model costs more time for parameter estimation. And our method achieves good cross-matching performance which is even better than that of VeriFinger 6.1 SDK-based method.

3). TPS model also achieves high accuracy of cross-matching, which proves its capability to describe the non-linear transformation. Its estimation depends on the initial minutiae correspondence, but it is difficult to pair minutiae for large-distorted fingerprints with traditional rigid model. In contrast, our algorithm iteratively expands the registration region to involve more minutiae and update/upgrade the model for the current region. This strategy ensures the current model is robust for the minutiae pairing in the newly expanded area.

4). At the stage of regular matching, EER of the VeriFinger 6.1 SDK-based method is 2-4 times lower than that of rigid model of our method. There are two factors due to the inequitable comparison. First, in the template generation stage, VeriFinger 6.1 SDK-based method adopts quality control. If the quality of input fingerprint image is lower than a threshold, the image will be discarded and its template can not be generated. So VeriFinger 6.1 SDK-based method discards some low quality fingerprint images and improves the matching performance on enrolled image databases. Second, in the matching stage, unlike our method uses only minutiae, VeriFinger 6.1 SDK-based method uses more features, which can also improve the matching performance.

Based on the above experimental results and analysis, we can conclude that our algorithms do contribute to the cross-matching performance improvement greatly evaluating from the comparison results in regular matching and cross-matching.

5. Conclusion

In this paper, a novel cross-matching algorithm is developed for the fingerprints from multi-type sensors. The main contributions of the proposed algorithm is the hierarchical registration process with model upgradation. The experimental results demonstrate that our algorithm achieves good performance in the cross-matching of fingerprints captured with four typical sensors.

In future, we will attempt to use the local features minutia-simplex or minutia-triplet to represent the fingerprint. They can strengthen the uniqueness of minutiae and improve the accuracy of feature pairing at the cost of matching time. We also consider involving some global features (texture or orientation) into cross-matching since global features are proved more robust for those partially captured fingerprints.

6. Acknowledgment

This paper is supported by Opening Fund of Top Key Discipline of Computer Software and Theory in Zhejiang Provincial Colleges at Zhejiang Normal University Grant No.ZSDZZZZXK36.

References

[1] A. E. Beaton and J. W. Tukey. The fitting of power series, meaning polynomials, illustrated on band-spectroscopic data. *Technometrics*, 16:147–185, 1974.

[2] K. Bubna and C. V. Stewart. Model selection techniques and merging rules for range data segmentation algorithms. *Computer Vision and Image Understanding*, 80(2):215–245, 2000.

[3] X. Chen, J. Tian, J. Cheng, and X. Yang. Segmentation of fingerprint images using linear classifier. *EURASIP*, 2004(4):480–494, 2004.

[4] L. Hong, Y. Wan, and A. K. Jain. Fingerprint image enhancement: algorithm and performance evaluation. *IEEE Trans. on Pattern Analysis and Machine Intelligence*, 20(8):777–789, 1998.

[5] X. Jia, X. Yang, Y. Zang, N. Zhang, and J. Tian. A cross-device matching fingerprint database from multi-type sensors. In *Proceedings of 21st International Conference on Pattern Recognition*, 2012.

[6] Z. M. Kovács-Vajna. A fingerprint verification system based on triangular matching and dynamic time warping. *IEEE Trans. on Pattern Analysis and Machine Intelligence*, 22(11):1266–1276, 2000.

[7] Z. M. Kovács-Vajna, R. Rovatti, and R. Frazzoni. Fingerprint ridge distance computation methodologies. *Pattern Recognition*, 33:69–80, 2000.

[8] X. Luo and J. Tian. Knowledge based fingerprint image enhancement. In *In Proceedings of 15th ICPR*, volume 4, pages 783–786.

[9] W. H. Press, S. A. Teukolsky, W. T. Vetterling, and B. P. Flannery. *Numerical recipes*. Third edition.

[10] A. Ross and A. K. Dass, S.and Jain. A deformable model for fingerprint matching. *Pattern Recognition*, 38(1):95–103, 2005.

[11] A. Ross and A. Jain. Biometric sensor interoperability: a case study in fingerprints. In *BioAW 2004, LNCS*, volume 3087, pages 134–145.

[12] A. Ross and R. Nadgir. A thin-plate spline calibration model for fingerprint sensor interoperability. *IEEE Trans. on Knowledge and Data Engineering*, 20(8):1097–1110, 2008.

[13] W. Sheng, G. Howells, M. C. Fairhurst, and F. Deravi. A memetic fingerprint matching algorithm. *IEEE Trans. on Information Forensics and Security*, 2(3):402–412, 2007.

[14] M. Tico and P. Kuosmanen. Fingerprint matching using an orientation-based minutia descriptor. *IEEE Trans. on Pattern Analysis and Machine Intelligence*, 25(8):1009–1014, 2003.

[15] VeriFinger. http://www.neurotechnology.com/verifinger.html.